All-dielectric reciprocal bianisotropic nanoparticles

Rasoul Alaee,[1,*] Mohammad Albooyeh,[2] Aso Rahimzadegan,[1] Mohammad S. Mirmoosa,[2]
Yuri S. Kivshar,[3] and Carsten Rockstuhl[1,4]

[1]*Institute of Theoretical Solid State Physics, Karlsruhe Institute of Technology, Karlsruhe 76131, Germany*
[2]*Department of Radio Science and Engineering, School of Electrical Engineering, Aalto University, Aalto, Finland*
[3]*Nonlinear Physics Centre, Research School of Physics and Engineering, Australian National University, Canberra ACT 0200, Australia*
[4]*Institute of Nanotechnology, Karlsruhe Institute of Technology, Karlsruhe 76021, Germany*

(Received 3 September 2015; revised manuscript received 18 November 2015; published 23 December 2015)

The study of high-index dielectric nanoparticles currently attracts a lot of attention. They do not suffer from absorption but promise to provide control of the properties of light comparable to plasmonic nanoparticles. To further advance the field, it is important to identify versatile dielectric nanoparticles with unconventional properties. Here, we show that breaking the symmetry of an all-dielectric nanoparticle leads to a geometrically tunable magnetoelectric coupling, i.e., an omega-type bianisotropy. The suggested nanoparticle exhibits different backscatterings and, as an interesting consequence, different optical scattering forces for opposite illumination directions. An array of such nanoparticles provides different reflection phases when illuminated from opposite directions. With a proper geometrical tuning, this bianisotropic nanoparticle is capable of providing a 2π phase change in the reflection spectrum while possessing a rather large and constant amplitude. This allows the creation of reflectarrays with near-perfect transmission out of the resonance band due to the absence of a usually employed metallic screen.

DOI: 10.1103/PhysRevB.92.245130 PACS number(s): 42.25.−p, 78.67.Bf, 45.20.da, 42.25.Fx

Nanophotonics has attracted enormous research interest due to its potential to control light-matter interaction at the nanoscale [1–4]. Being usually connected with a strong light confinement in metal-dielectric and plasmonic structures, nanophotonics offers remarkable opportunities due to the local field enhancement [5–7]. However, applications of plasmonic nanophotonics are often limited by Ohmic losses at optical frequencies [8–12]. An alternative strategy in nanophotonics is to use high-index dielectric materials for building blocks that control light-matter interaction [13–15]. Dielectric nanoparticles have attracted considerable attention due to their appealing applications [16–22].

For these nanoparticles to be versatile, usually the multipolar composition of their scattered field is tailored. A high-index dielectric nanoparticle that supports both electric and magnetic resonant responses, where the exact composition of the two contributions can be tuned by means of geometrical modifications, has been recently suggested [23–25]. Interesting optical features such as directional scattering pattern with zero backscattering or an optical pulling force can be achieved by proper tuning of these responses [26–30]. Nanoparticles with higher multipolar responses, e.g., electric and magnetic quadrupoles may provide even more control of the scattering properties [31,32] when compared to nanoparticles with only dipolar responses. However, they require more complicated theoretical considerations and a range of dissimilar materials [32]. Therefore, it is a challenge to bring more control of the scattering features of nanoparticles without adding such complexities. Here, we use *bianisotropy* to control the scattering properties of high-index dielectric nanoparticles in the context of *dipolar* responses [33,34]. Note that we are only interested in the reciprocal omega-type bianisotropy, and all the other types of bianisotropy (i.e., chiral, Tellegen, and moving) are absent [33,35]. We show that an omega-type bianisotropic response can be achieved by breaking the symmetry of a cylindrical nanoparticle, i.e., a high-index dielectric cylinder with a partially drilled cylindrical air hole [see Figs. 1(a) and 1(b)].

A reciprocal omega-type bianisotropic nanoparticle supports electric and magnetic dipole moments with different strength when illuminated by a plane wave in the forward or backward direction [see Fig. 1(a)]. In particular, the bianisotropy causes significant difference in backscattering responses and consequently in the optical scattering forces exerted on the proposed nanoparticle for opposite illumination directions. The observed magnetoelectric coupling can be tuned by controlling geometric parameters of the nanoparticle. We demonstrate that an infinite periodic planar array of such lossless nanoparticles (a metasurface), provides different *resonant* reflection phases for different illumination directions. This is due to the proposed magnetoelectric coupling, and it is certainly not possible with only an electric and/or magnetic response. We also demonstrate that the investigated nanoparticle is an excellent candidate for unit cells of reflectarrays. Indeed, this nanoparticle in its reflection resonance band provides a 2π phase change for a proper geometrical tuning while it maintains a considerably large and constant amplitude, similar to Huygens' metasurfaces [36]. Moreover, since there is no metallic ground plate in the proposed reflectarray, it will be transparent out of its resonance band.

I. BIANISOTROPIC NANOPARTICLES

The geometry of the proposed bianisotropic high-index dielectric nanoparticle is shown in Figs. 1(a) and 1(b). The suggested nanoparticle is not symmetric with respect to the forward and backward illumination directions [see Fig. 1(a)]. Material and geometric parameters of the nanoparticle are

*Corresponding author: rasoul.khanghah@kit.edu

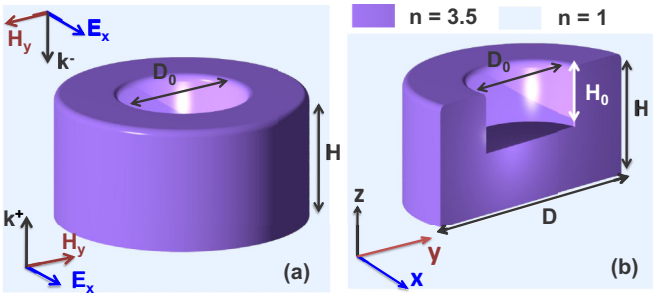

FIG. 1. (Color online) (a) Schematic of the proposed bianisotropic high-index dielectric nanoparticle. (b) A cut in the yz-plane of the proposed nanonatenna. The dielectric cylinder has a diameter $D = 300$ nm and height $H = 150$ nm with a cylindrical hole inside it that has a diameter $D_0 = 150$ nm and height $H_0 = 10$–140 nm. We assumed that the refractive index of the material from which the cylinder is made is $n = 3.5$. The ambient material shall be air with a refractive index of unity.

given in Fig. 1. Using the multipole expansion of the scattered field [37], we compute the total scattering cross section and the contribution of each multipole moment when the nanoparticle is illuminated by a plane wave in the forward and backward directions [see Figs. 2(a) and 2(c)]. The higher order multipole moments, i.e., electric quadrupole Q and magnetic quadrupole QM moments are negligible below 450 THz [the frequency range above 450 THz is marked by the gray shadowed areas in Figs. 2(a) and 2(c)]. In the following, we only concentrate on this frequency range (i.e., lower than 450 THz where only

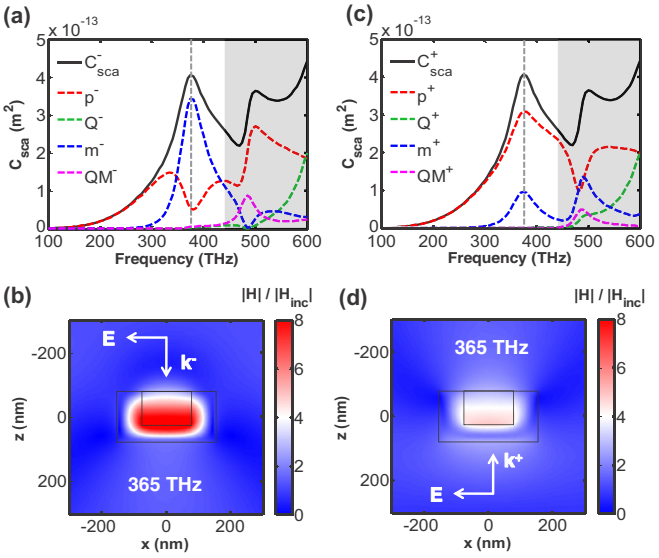

FIG. 2. (Color online) (a) and (c) Total scattering cross sections $C_{sca}^{\pm}$ and contributions from different Cartesian multipole moments as a function of frequency for forward (+) and backward (−) illumination directions; electric dipole moment $p^{\pm}$ (red dashed line), magnetic dipole moment $m^{\pm}$ (blue dashed line), electric quadrupole moment $Q^{\pm}$ (green dashed line), and magnetic quadrupole moment $QM^{\pm}$ (purple dashed line). The height of the air hole is $H_0 = 100$ nm. (b) and (d) normalized magnetic field distributions at 365 THz [gray dashed line in (a) and (c)] for both opposite illumination directions.

electric and magnetic dipole moments are dominant). The corresponding electric $p_x^{\pm}$ and magnetic $m_y^{\pm}$ dipole moments of the nanoparticle for both illumination directions (see Fig. 1) are given by:

$$\frac{p_x^{\pm}}{\epsilon_0} = \alpha_{ee} E_x^{inc} \pm \alpha_{em} Z_0 H_y^{inc}, \tag{1}$$

$$Z_0 m_y^{\pm} = \alpha_{me} E_x^{inc} \pm \alpha_{mm} Z_0 H_y^{inc}, \tag{2}$$

where ϵ_0 is the free space permittivity and Z_0 is the characteristic impedance of free space. α_{ee}, α_{em}, α_{me}, and α_{mm} are individual polarizabilities of the nanoparticle. They represent electric, magnetoelectric, electromagnetic, and magnetic couplings in the proposed nanoparticle, respectively, that is, the interactions between the electric and magnetic fields and polarizations [33,38]. Notice that in order to distinguish the illumination direction of the nanoparticle, we use the ± sign where the plus/minus sign corresponds to the propagation direction of the incident plane waves in the forward/backward direction (the time dependency is assumed to be $e^{-i\omega t}$). In order to explain the underlying physical mechanisms of the scattering response of the bianisotropic nanoparticle, we start with the definition of extinction cross section $C_{ext}^{\pm}$ for a bianisotropic nanoparticle in dipole approximation for both illumination directions, i.e., [1,39,40]

$$\begin{aligned} C_{ext}^{\pm} &= \frac{P_{ext}^{\pm}}{I_0} \\ &= \frac{-\frac{1}{2}\mathrm{Re}\oiint_S (\mathbf{E}_{inc} \times \mathbf{H}_{sca}^{\pm *} + \mathbf{E}_{sca}^{\pm} \times \mathbf{H}_{inc}^{*}) \cdot \mathbf{n} ds}{I_0} \\ &= k\mathrm{Im}(\alpha_{ee} \pm \alpha_{em} \pm \alpha_{me} + \alpha_{mm}), \end{aligned} \tag{3}$$

where $I_0 = |\mathbf{E}_{inc}|/2Z_0$ is the intensity of the incident plane wave. $|\mathbf{E}_{inc}|$ and $|\mathbf{E}_{sca}^{\pm}|$ are the amplitude of the incident and scattered electric fields for both illumination directions (±). $P_{ext}^{\pm}$ is the extracted power by the nanoparticle, and $k = \omega/c$ is the wave number for an angular frequency ω. For a reciprocal nanoparticle [33], i.e., $\alpha_{em} = -\alpha_{me}$, we can conclude that the extinction cross section for both illuminations are identical, i.e., $C_{ext} = C_{ext}^{+} = C_{ext}^{-}$ and is given by

$$C_{ext} = k\mathrm{Im}(\alpha_{ee} + \alpha_{mm}), \tag{4}$$

On the other hand, we know for the proposed nanoparticle that the scattering cross sections for both illuminations can be written as [1,39,40]

$$\begin{aligned} C_{sca}^{\pm} &= \frac{P_{sca}^{\pm}}{I_0} \\ &= \frac{\frac{1}{2}\mathrm{Re}\oiint_S (\mathbf{E}_{sca}^{\pm} \times \mathbf{H}_{sca}^{\pm *}) \cdot \mathbf{n} ds}{I_0} \\ &= \frac{k^4}{6\pi}(|\alpha_{ee} \pm \alpha_{em}|^2 + |\alpha_{me} \pm \alpha_{mm}|^2), \end{aligned} \tag{5}$$

where $P_{sca}^{\pm}$ is the radiated or scattered power by the nanoparticle. The extinction cross section C_{ext} for a lossless reciprocal nanoparticle is identical to the scattering cross section C_{sca}, i.e., $C_{ext} = C_{sca}$ due to the fact that the absorption cross section is zero $C_{abs} = C_{ext} - C_{sca} = 0$. This explains why the scattering cross sections are identical for the proposed

nanoparticle when illuminated from opposite directions, i.e., $C_{sca} = C^{+}_{sca} = C^{-}_{sca}$ [see black solid lines in Figs. 2(a) and 2(c)]. Notice, the equality between extinction and scattering cross sections for the lossless bianisotropic nanoparticle leads to an expression known as the Sipe-Kranendonk condition [40–43]. It is important to note that for a plasmonic bianisotropic nanoparticle, due to the intrinsic Ohmic losses of metals, the scattering and absorption cross sections will be different for forward and backward illuminations [34,44]. Furthermore, a planar periodic array of lossy bianisotropic nanoparticles possesses interesting optical features such as strongly asymmetric reflectance and perfect absorption. These effects have been studied before [34,45]. Although the scattering/extinction cross sections are similar for different illumination directions in the proposed nanoparticle, the contributions of the electric and magnetic dipole moments to the total scattering cross sections are not, i.e., $p^{+}_{x} \neq p^{-}_{x}$ and $m^{+}_{y} \neq m^{-}_{y}$ [see red and blue dashed lines in Figs. 2(a) and 2(c)]. It can also be seen from Figs. 2(b) and 2(d) that the magnetic field distributions are significantly different when the nanoparticle is illuminated from the forward and backward directions. This is obviously due to the presence of magnetoelectric coupling, which is introduced by the asymmetry in the nanoparticle.

In order to prove this, we have also calculated the individual polarizability components of the nanoparticle [see Figs. 3(a)–3(c)] [34,37,46,47]. The magnetoelectric coupling α_{em} is comparable with the electric α_{ee} and magnetic α_{mm} couplings for the proposed nanoparticle [see Figs. 3(a)–3(c)]. The level of this coupling can be tuned by changing the geometrical parameters of the nanoparticle, i.e., the height H_0 or the diameter D_0 of the partially drilled cylindrical air hole inside the high-index dielectric cylinder. Figure 3(d) presents the magnitude of electric, magnetic, and magnetoelectric polarizabilities of the nanoparticle at the maximum of magnetoelectric coupling ($|\alpha_{em}|^{max}$) as a function of the height of the cylindrical air hole H_0. It confirms that the amplitude of the magnetoelectric coupling can be tuned, and its maximum occurs when the height of the hole H_0 is appropriately half the height of the dielectric cylinder H, i.e., $H_0 \approx \frac{H}{2} = 75$ nm. Notice, the magnetoelectric coupling can also be tuned by changing the diameter of cylindrical air hole D_0 (not shown for the sake of brevity).

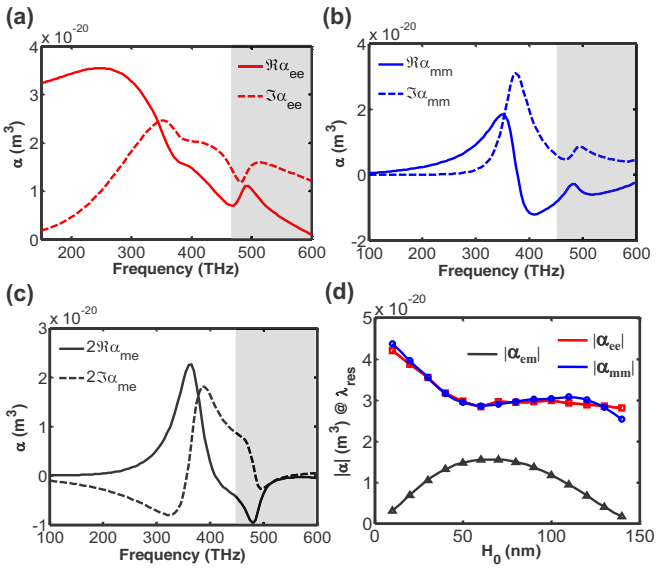

FIG. 3. (Color online) (a)–(c) Individual polarizability components of the proposed nanoparticle. The geometrical parameters are: the height of the cylinder $H = 150$ nm, the height of the cylindrical air hole $H_0 = 100$ nm, and its diameter $D_0 = 150$ nm. (d) Amplitude of the individual polarizability components at the maximum of the magnetoelectric coupling as a function of H_0. The maximum bianisotropy happens when the height of the air hole is approximately half of the height of the dielectric cylinder, i.e., $H_0 \approx \frac{H}{2} = 75$ nm.

As highlighted before, a lossless bianisotropic nanoparticle possesses identical scattering cross sections for both forward and backward illumination directions. Moreover, the forward radar cross sections as shown in Fig. 4(a) are identical for both illumination directions according to the definition of the normalized forward radar cross section [34]:

$$\begin{aligned} Q^{\pm}_{RFS} &= \lim_{r\to\infty} \frac{4\pi r^2}{A} \frac{|\mathbf{E}_{sca}(\varphi = 0, \theta^{\pm} = 0, \pi)|^2}{|\mathbf{E}_{inc}|^2} \\ &= \frac{k^4}{4\pi A} |\alpha_{ee} \pm \alpha_{em} \pm \alpha_{me} + \alpha_{mm}|^2 \\ &= \frac{k^4}{4\pi A} |\alpha_{ee} + \alpha_{mm}|^2. \end{aligned} \tag{6}$$

However, the backward radar cross section depends on the illumination directions [see Fig. 4(a)]. It measures the share of light that is directly back reflected. In order to show that, we start with the definition of the normalized backward radar cross section for both illuminations $Q^{\pm}_{RBS}$, i.e., the backward radar cross section divided by the geometrical cross section [34]

$$\begin{aligned} Q^{\pm}_{RBS} &= \lim_{r\to\infty} \frac{4\pi r^2}{A} \frac{|\mathbf{E}_{sca}(\varphi = 0, \theta^{\pm} = \pi, 0)|^2}{|\mathbf{E}_{inc}|^2} \\ &= \frac{k^4}{4\pi A} |\alpha_{ee} \mp \alpha_{em} \pm \alpha_{me} - \alpha_{mm}|^2, \end{aligned} \tag{7}$$

where $A = \pi(D/2)^2$ is the geometrical cross section and D is the diameter of the nanoparticle (see Fig. 1). Therefore, for the reciprocal nanoparticle, i.e., $\alpha_{em} = -\alpha_{me}$, the normalized backward radar cross section $Q^{\pm}_{RBS}$ can be written as [34]

$$Q^{\pm}_{RBS} = \frac{k^4}{4\pi A} |\alpha_{ee} \mp 2\alpha_{em} - \alpha_{mm}|^2. \tag{8}$$

Consequently, due to bianisotropy, the backscattering responses $Q^{\pm}_{RBS}$ are significantly different when the nanoparticle is illuminated from opposite directions [see Fig. 4(a)]. Hence, the nanoparticle possesses different radiation patterns for both illumination directions as depicted in Figs. 4(b) and 4(c).

The dominant effect of the backscattering on optical scattering forces is shown for a dipolar particle without a magnetoelectric response [48]. Since the investigated bianisotropic nanoparticle shows a notable backscattering difference, it is interesting to explore the optical scattering forces in the realm of the bianisotropic particles.

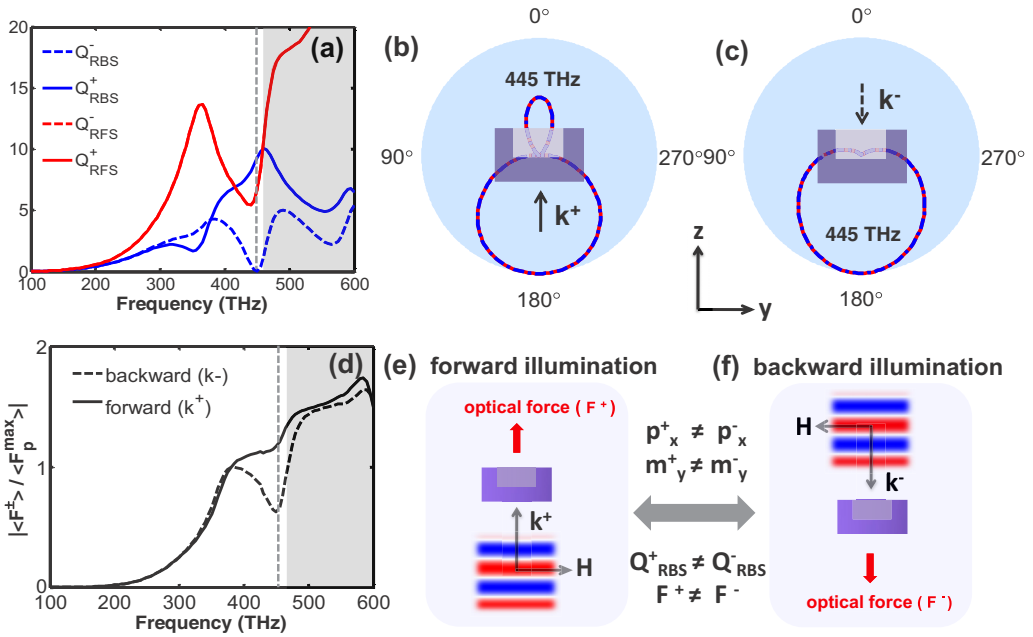

FIG. 4. (Color online) (a) Normalized backward (blue lines) and forward (red lines) radar cross sections when the nanoparticle is illuminated from backward (dashed lines) and forward (solid lines) directions for $H_0 = 75$ nm. Note that the forward radar cross sections are identical and hence indistinguishable in the figure. (b) Radiation patterns for forward and (c) backward illumination directions at 445 THz, respectively. (d) Normalized forward (solid lines) and backward (dashed lines) optical forces. $F_p^{\max} = \frac{3\pi}{k^2}\epsilon_0|\mathbf{E}_{\rm inc}|^2$ is the maximum force applied on a particle which exhibits an electric dipole moment with an incidence plane wave. (e) Schematic view of the different illuminations for forward and (f) backward illumination directions.

The optical scattering force on a dipolar particle for a plane wave incident field reads as [27]

$$\langle \mathbf{F} \rangle = \frac{1}{2}\mathrm{Re}(\nabla \mathbf{E}^*_{\rm inc}\cdot\mathbf{p}) + \frac{1}{2}\mu_0\mathrm{Re}(\nabla \mathbf{H}^*_{\rm inc}\cdot\mathbf{m}) - \frac{k^4}{12\pi\epsilon_0 c}\mathrm{Re}(\mathbf{p}\times\mathbf{m}^*). \quad (9)$$

Plugging Eqs. (1) and (2) into Eq. (9), one drives the optical scattering force for both illuminations:

$$\langle \mathbf{F}^{\pm} \rangle = \pm\mathbf{e}_z\frac{k}{2}\epsilon_0\left|E_{\rm x}^{\rm inc}\right|^2\left\{\mathrm{Im}(\alpha_{\rm ee}\pm\alpha_{\rm em})\pm\mathrm{Im}(\alpha_{\rm me}\pm\alpha_{\rm mm}) \mp\frac{k^3}{6\pi}\mathrm{Re}[(\alpha_{\rm ee}\pm\alpha_{\rm em})(\alpha_{\rm me}\pm\alpha_{\rm mm})^*]\right\}. \quad (10)$$

The difference between the forces applied on the nanoparticle in the direction of propagation assuming $\alpha_{\rm em} = -\alpha_{\rm me}$ (reciprocity) leads to

$$\triangle F = |\langle \mathbf{F}^+\rangle| - |\langle \mathbf{F}^-\rangle| = \frac{k^4}{6\pi}\epsilon_0\left|E_{\rm x}^{\rm inc}\right|^2\mathrm{Re}(\alpha_{\rm em}\alpha^*_{\rm mm} - \alpha_{\rm ee}\alpha^*_{\rm em}). \quad (11)$$

Equation (11) shows that the magnetoelectric polarizability can lead to different optical scattering forces for opposite illuminations. Figure 4(d) shows the normalized optical scattering forces. It can be seen that $\triangle F$ is pronounced when the nanoparticle exhibits a notable difference in backward radar cross sections (i.e., at 445 THz).

In summary, the following relations hold for the proposed lossless reciprocal bianisotropic nanoparticle:

$$p^+ \neq p^-, \quad m^+ \neq m^-, \quad C_{\rm sca} = C_{\rm ext} = C^{\pm}_{\rm scat} = C^{\pm}_{\rm ext}, \quad Q^+_{\rm RFS} = Q^-_{\rm RFS}, \quad Q^+_{\rm RBS} \neq Q^-_{\rm RBS}, \quad |\langle \mathbf{F}^+\rangle| \neq |\langle \mathbf{F}^-\rangle|. \quad (12)$$

Now we finish the investigations of the properties of the individual nanoparticle and start to demonstrate its interesting characteristics when used in a planar periodic array.

II. BIANISOTROPIC METASURFACES

Next, we consider a periodic array composed of the proposed bianisotropic nanoparticle that is arranged along a planar surface, here the xy plane [see Fig. 5(a)]. Since the nanoparticles are assumed to be lossless, the Ohmic losses of the proposed array are also zero. Let us illuminate this array at normal incidence from two directions, i.e., forward and backward direction [see Fig. 5(a) for the definition of forward and backward illumination]. The reflection and transmission amplitudes and phases for these two illumination cases are plotted in Figs. 5(b) and 5(c). They were obtained from full wave simulations using COMSOL Multiphysics [49]. It is obvious that the amplitudes for the reflection and transmission for the different illumination directions are identical since there are no losses. The transmission phase is identical due to reciprocity. On the contrary, the reflection phase is not. This is apparently due to the presence of bianisotropy in the proposed array.

Now, we claim that the proposed nanoparticle is a proper candidate as a unit cell in a reflectarray. Indeed, a unit cell

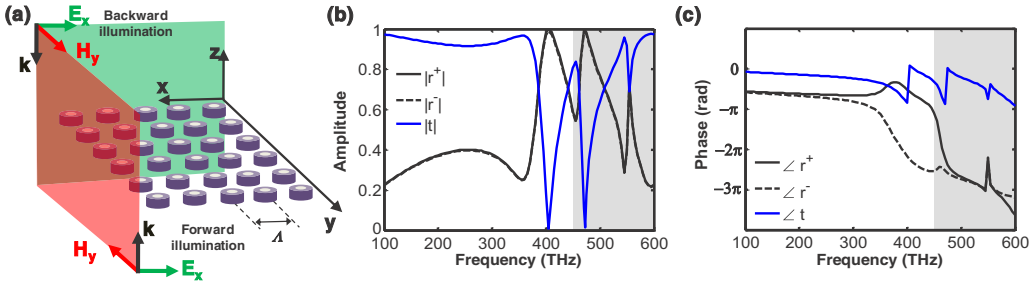

FIG. 5. (Color online) (a) A metasurface composed of an array of bianisotropic nanoparticles with $H_0 = 75$ nm. (b) Reflection and transmission amplitude for two illumination directions shown in (a). (c) The same plots as in (b) but for the corresponding phases. The reference plane for the phases is considered at the $z = 0$ plane.

must provide a 2π phase change prior to being applicable in a reflectarray [36,50–53]. This 2π phase change shall be obtained by a suitable geometrical tuning. Moreover, it has to maintain a high reflection amplitude across the considered geometrical configuration. Figure 6 shows the amplitude and phase variations versus different height and diameter of the air hole inside the dielectric cylinder when the proposed nanoparticle is used in a square array with period $\Lambda = 400$ nm.

As can be seen from Fig. 6(a), the proposed nanoparticle satisfies the required condition for the phase variation of the reflection coefficient for both illumination directions when we fix the height $H_0 = 75$ nm and change the diameter $D_0 =$ 20–280 nm. The amplitude of the reflection coefficient is close to unity within an acceptable range, while it drops down to one half at both ends of the diameter variations. The situation is a bit worse for the case when we fix the diameter $D_0 =$ 150 nm and vary the height $H_0 =$ 10–140 nm. In this case, we obtain a phase variation of 2π only for the forward illumination direction, while the amplitude of the reflection coefficient, in some parameter regions, drops down to 20% [see Fig. 6(b)]. We should mention that better results might be obtained if the geometry is carefully optimized. The presented example only serves the purpose of demonstrating the idea.

Another important point is that the proposed nanoparticles in the array provide asymmetric phase variations. That is, the variation of reflection phases are different for different illumination directions. It means that we may properly design a reflectarray with two different properties when looking from different directions onto the plane. This is impossible using symmetrical structures which do not have bianisotropic properties.

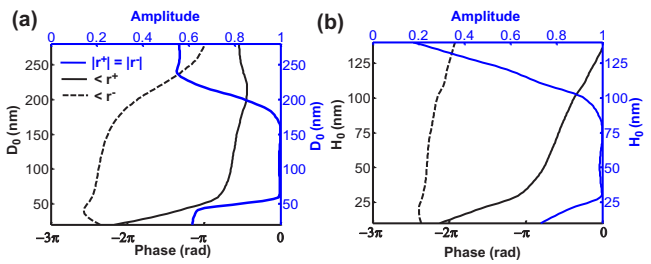

FIG. 6. (Color online) (a) Phase-change curve for the reflection coefficient of an array of nanoparticles versus the diameter of the air hole at resonance frequency $f = 405$ THz for two different illumination directions denoted by r^+ and r^-. H_0 is fixed to 75 nm. (b) The same plot as in (a) for variation of air hole height. D_0 is fixed to 150 nm.

The most important point about the proposed reflectarray is its transparency out of the resonance band. Indeed, in the investigated reflectarray, we do not rely on a metallic back reflector [52,54,55]. Instead, we have offered resonant nanoparticles with bianisotropic properties to obtain a full reflection. This gives us the possibility to preserve transparency outside the resonance band in the reflectarray. This transparency is very important when combining multiple receiving/transmitting systems. Then, we need a reflectarray at a frequency band, while we do not want to prevent signals from getting transmitted out of that frequency band.

III. CONCLUSIONS

We have proposed a design for high-index dielectric nanoparticle which supports an omega-type bianisotropic coupling in addition to magnetic and electric optically-induced dipole resonances. We have demonstrated that the magnetoelectric coupling can be tuned by geometric parameters of the nanoparticle. In particular, the nanoparticle can possess different backward cross sections and consequently different optical scattering forces, when being illuminated by a plane wave from opposite directions along with the identical forward cross sections.

For a metasurface created by a periodic array of bianisotropic nanoparticles, we have observed interesting effects, e.g., asymmetric reflection phases for the opposite illumination directions and a possibility to achieve a 2π phase change together with an acceptable reflection amplitude across the entire phase spectrum by tuning the geometric parameters of the nanoparticle. Finally, we have demonstrated that the employment of the proposed resonant nanoparticle together with the absence of a fully reflective metallic screen gives the opportunity of *out-of-band transparency* in reflectarrays. All the effects described here are the direct outcome of the engineered omega-type bianisotropy that may open a path to design high-index nanoparticles and metasurfaces, including reflectarrays, transmitarrays, and Huygens metasurfaces.

ACKNOWLEDGMENTS

The authors thank the German Science Foundation (project RO 3640/7-1) for financial support. The work was also supported by the DAAD (PPP Australien) and the Australian Research Council.

[1] L. Novotny and B. Hecht, *Principles of Nano-Optics* (Cambridge University Press, New York, 2006).

[2] S. A. Maier, *Plasmonics: Fundamentals and Applications* (Springer, New York, 2007).

[3] D. K. Gramotnev and S. I. Bozhevolnyi, Nat. Photon. **4**, 83 (2010).

[4] H. A. Atwater and A. Polman, Nat. Mater. **9**, 205 (2010).

[5] J. A. Schuller, E. S. Barnard, W. Cai, Y. C. Jun, J. S. White, and M. L. Brongersma, Nat. Mater. **9**, 193 (2010).

[6] M. Albooyeh and C. R. Simovski, Opt. Express **20**, 21888 (2012).

[7] R. Alaee, C. Menzel, U. Huebner, E. Pshenay-Severin, S. Bin Hasan, T. Pertsch, C. Rockstuhl, and F. Lederer, Nano Lett. **13**, 3482 (2013).

[8] A. Boltasseva and H. A. Atwater, Science **331**, 290 (2011).

[9] P. Tassin, T. Koschny, M. Kafesaki, and C. M. Soukoulis, Nat. Photon. **6**, 259 (2012).

[10] D. S. Filonov, A. E. Krasnok, A. P. Slobozhanyuk, P. V. Kapitanova, E. A. Nenasheva, Y. S. Kivshar, and P. A. Belov, Appl. Phys. Lett. **100**, 201113 (2012).

[11] P. Moitra, Y. Yang, Z. Anderson, I. I. Kravchenko, D. P. Briggs, and J. Valentine, Nat. Photon. **7**, 791 (2013).

[12] R. Alaee, R. Filter, D. Lehr, F. Lederer, and C. Rockstuhl, Opt. Lett. **40**, 2645 (2015).

[13] A. Ahmadi and H. Mosallaei, Phys. Rev. B **77**, 045104 (2008).

[14] A. B. Evlyukhin, C. Reinhardt, A. Seidel, B. S. Luk'yanchuk, and B. N. Chichkov, Phys. Rev. B **82**, 045404 (2010).

[15] A. B. Evlyukhin, S. M. Novikov, U. Zywietz, R. L. Eriksen, C. Reinhardt, S. I. Bozhevolnyi, and B. N. Chichkov, Nano Lett. **12**, 3749 (2012).

[16] A. E. Krasnok, A. E. Miroshnichenko, P. A. Belov, and Y. S. Kivshar, Opt. Express **20**, 20599 (2012).

[17] Y. Yang, I. I. Kravchenko, D. P. Briggs, and J. Valentine, Nat. Commun. **5**, 5753 (2014).

[18] A. E. Krasnok, P. A. Belov, A. E. Miroshnichenko, A. I. Kuznetsov, B. S. Luk'yanchuk, and Y. S. Kivshar, arXiv:1411.2768.

[19] M. L. Brongersma, Y. Cui, and S. Fan, Nat. Mater. **13**, 451 (2014).

[20] D. Lin, P. Fan, E. Hasman, and M. L. Brongersma, Science **345**, 298 (2014).

[21] I. Staude, V. V. Khardikov, N. T. Fofang, S. Liu, M. Decker, D. N. Neshev, T. S. Luk, I. Brener, and Y. S. Kivshar, ACS Photonics **2**, 172 (2015).

[22] A. Jain, P. Tassin, T. Koschny, and C. M. Soukoulis, Phys. Rev. Lett. **112**, 117403 (2014).

[23] J. A. Schuller, R. Zia, T. Taubner, and M. L. Brongersma, Phys. Rev. Lett. **99**, 107401 (2007).

[24] A. I. Kuznetsov, A. E. Miroshnichenko, Y. H. Fu, J. Zhang, and B. Lukyanchuk, Sci. Rep. **2**, 492 (2012).

[25] I. Staude, A. E. Miroshnichenko, M. Decker, N. T. Fofang, S. Liu, E. Gonzales, J. Dominguez, T. S. Luk, D. N. Neshev, I. Brener *et al.*, ACS Nano **7**, 7824 (2013).

[26] M. Kerker, D.-S. Wang, and C. L. Giles, J. Opt. Soc. Am. **73**, 765 (1983).

[27] J. Chen, J. Ng, Z. Lin, and C. T. Chan, Nat. Photon. **5**, 531 (2011).

[28] J. J. Saenz, Nat. Photon **5**, 514 (2011).

[29] X. Zambrana-Puyalto, I. Fernandez-Corbaton, M. L. Juan, X. Vidal, and G. Molina-Terriza, Opt. Lett. **38**, 1857 (2013).

[30] S. Person, M. Jain, Z. Lapin, J. J. Saenz, G. Wicks, and L. Novotny, Nano Lett. **13**, 1806 (2013).

[31] W. Liu, J. Zhang, B. Lei, H. Ma, W. Xie, and H. Hu, Opt. Express **22**, 16178 (2014).

[32] A. Mirzaei, A. E. Miroshnichenko, I. V. Shadrivov, and Y. S. Kivshar, Sci. Rep. **5**, 9574 (2015).

[33] A. Serdyukov, *Electromagnetics of Bi-anisotropic Materials: Theory and Applications*, Vol. 11 (Taylor & Francis, Amsterdam, 2001).

[34] R. Alaee, M. Albooyeh, M. Yazdi, N. Komjani, C. Simovski, F. Lederer, and C. Rockstuhl, Phys. Rev. B **91**, 115119 (2015).

[35] A. Priou, A. Sihvola, S. Tretyakov, and A. Vinogradov, *Advances in Complex Electromagnetic Materials*, Vol. 28 (Springer Science & Business Media, Dordrecht, 2012).

[36] M. Decker, I. Staude, M. Falkner, J. Dominguez, D. N. Neshev, I. Brener, T. Pertsch, and Y. S. Kivshar, Adv. Opt. Mater. **3**, 813 (2015).

[37] S. Mühlig, C. Menzel, C. Rockstuhl, and F. Lederer, Metamaterials **5**, 64 (2011).

[38] M. Albooyeh and C. Simovski, J. Opt. **13**, 105102 (2011).

[39] C. F. Bohren and D. R. Huffman, *Absorption and Scattering of Light by Small Particles* (Wiley-VCH, New York, 1998).

[40] P. Belov, S. Maslovski, K. Simovski, and S. Tretyakov, Tech. Phys. Lett. **29**, 718 (2003).

[41] J. E. Sipe and J. V. Kranendonk, Phys. Rev. A **9**, 1806 (1974).

[42] S. Tretyakov, *Analytical Modeling in Applied Electromagnetics* (Artech House, Boston, 2003).

[43] I. Sersic, M. A. van de Haar, F. B. Arango, and A. F. Koenderink, Phys. Rev. Lett. **108**, 223903 (2012).

[44] D. L. Sounas and A. Alu, Opt. Lett. **39**, 4053 (2014).

[45] C. Menzel, C. Helgert, C. Rockstuhl, E.-B. Kley, A. Tünnermann, T. Pertsch, and F. Lederer, Phys. Rev. Lett. **104**, 253902 (2010).

[46] Y. E. Terekhov, A. Zhuravlev, and G. Belokopytov, Moscow Univ. Phys. Bull. (Engl. Transl.) **66**, 254 (2011).

[47] F. Bernal Arango, T. Coenen, and A. F. Koenderink, ACS Photonics **1**, 444 (2014).

[48] M. Nieto-Vesperinas, R. Gomez-Medina, and J. J. Saenz, J. Opt. Soc. Am. A **28**, 54 (2011).

[49] COMSOL Multiphysics 4.3 User's Guide (2012).

[50] J. Huang, *Reflectarray Antenna* (Wiley Online Library, New York, 2005).

[51] M. Albooyeh, N. Komjani, and M. S. Mahani, Antennas and Wireless Propagation Letters, IEEE **8**, 319 (2009).

[52] A. V. Kildishev, A. Boltasseva, and V. M. Shalaev, Science **339**, 6125 (2013).

[53] J. Cheng, D. Ansari-Oghol-Beig, and H. Mosallaei, Opt. Lett. **39**, 6285 (2014).

[54] M. Farmahini-Farahani and H. Mosallaei, Opt. Lett. **38**, 462 (2013).

[55] N. Yu and F. Capasso, Nat. Mater. **13**, 139 (2014).